

# Overview Of ERA Integrated Technology Demonstration (ITD) 51A Ultra-High Bypass (UHB) Integration for Hybrid Wing Body (HWB)

Jeffrey D. Flamm\*

*NASA Langley Research Center, Hampton, VA 23681, USA*

Kevin D. James†

*NASA Ames Research Center, Moffett Field, CA 94035, USA*

John T. Bonet‡

*The Boeing Company, Huntington Beach, CA 92647, USA*

The NASA Environmentally Responsible Aircraft Project (ERA) was a five year project broken into two phases. In phase II, high N+2 Technical Readiness Level demonstrations were grouped into Integrated Technology Demonstrations (ITD). This paper describes the work done on ITD-51A: the Vehicle Systems Integration, Engine Airframe Integration Demonstration. Refinement of a Hybrid Wing Body (HWB) aircraft from the possible candidates developed in ERA Phase I was continued. Scaled powered, and unpowered wind-tunnel testing, with and without acoustics, in the NASA LARC 14- by 22-foot Subsonic Tunnel, the NASA ARC Unitary Plan Wind Tunnel, and the 40- by 80-foot test section of the National Full-Scale Aerodynamics Complex (NFAC) in conjunction with very closely coupled Computational Fluid Dynamics was used to demonstrate the fuel burn and acoustic milestone targets of the ERA Project.

## Nomenclature

$\alpha$	Angle-of-Attack
AEDC	Arnold Engineering Development Center
ARC	Ames Research Center
ARMD	Aeronautics Research Mission Directorate
AVC	Advanced Vehicle Concept
$\beta$	Angle-of-Sideslip
CFD	Computational Fluid Dynamics
EAI	Engine Airframe Integration
FOD	Foreign Object Damage
FTN	Flow Through Nacelle
HWB	Hybrid Wing Body
ISRP	Integrated Systems Research Program
LaRC	Langley Research Center
M	Mach Number
NASA	National Aeronautics and Space Administration
NFAC	National Full-Scale Aerodynamics Complex
OML	Outer Mold Line

---

\*Aerospace Engineer, Configuration Aerodynamics Branch, Mail Stop 499, AIAA Associate Fellow.

†Aerospace Engineer, Experimental Aero-Physics Branch, Mail Stop 260-1, AIAA Associate Fellow.

‡Aerodynamics Engineer, Boeing Research & Technology, 14900 Bolsa Chica Rd., AIAA Senior Member.

PSC	Preferred System Concept
psf	Pound per square foot
$q_\infty$	Dynamic Pressure
TPS	Turbine Propulsion Simulator
TRL	Technical Readiness Level
UHB	Ultra High By-Pass
UPWT	Unitary Plan Wind Tunnel
VSI	Vehicle Systems Integration

## I. Introduction

THE Environmentally Responsible Aviation (ERA) Project within the Integrated Systems Research Program (ISRP) of the NASA Aeronautics Research Mission Directorate (ARMD) had the responsibility to explore and document the feasibility, benefits, and technical risk of air vehicle concepts and enabling technologies that to reduce the impact of aviation on the environment. The primary goal of the ERA Project was to select air vehicle concepts and technologies that could simultaneously reduce fuel burn, noise, and emissions. In addition, the ERA Project identified and mitigated technical risk and transferred knowledge to the aeronautics community at large so that new technologies and vehicle concepts could be incorporated into the future design of aircraft. ERA was to address aircraft performance (especially “green” technology) within the N+2 (2020) timeframe for entry into service with the objective of integrating the most viable current TRL (1-4) technologies and bridging the gap up to TRL of 6. The current NASA subsonic transport system level metrics table is shown in figure 1.

v2013.1

TECHNOLOGY BENEFITS*	TECHNOLOGY GENERATIONS (Technology Readiness Level = 4-6)		
	N+1 (2015)	N+2 (2020**)	N+3 (2025)
Noise (cum margin rel. to Stage 4)	-32 dB	-42 dB	-52 dB
LTO NOx Emissions (rel. to CAEP 6)	-60%	-75%	-80%
Cruise NOx Emissions (rel. to 2005 best in class)	-55%	-70%	-80%
Aircraft Fuel/Energy Consumption† (rel. to 2005 best in class)	-33%	-50%	-60%

\* Projected benefits once technologies are matured and implemented by industry. Benefits vary by vehicle size and mission. N+1 and N+3 values are referenced to a 737-800 with CFM56-7B engines, N+2 values are referenced to a 777-200 with GE90 engines

\*\* ERA's time-phased approach includes advancing "long-pole" technologies to TRL 6 by 2015

† CO2 emission benefits dependent on life-cycle CO2e per MJ for fuel and/or energy source used

Figure 1: NASA subsonic transport system level metrics.

The focus of this paper is the Ultra-High Bypass Ratio (UHB) Engine integration for Hybrid Wing Body technology demonstration located within the ERA Vehicle Systems Integration sub project. This technology demonstration addresses the ERA technical challenge to *Demonstrate reduced component noise signatures leading to 42 EPNdB to Stage 4 noise margin for the aircraft system while minimizing weight and integration penalties to enable 50 percent fuel burn reduction at the aircraft system level.*

This Ultra-High Bypass (UHB) Ratio Engine integration for Hybrid Wing Body technology demonstration seeks to quantify the impact of engine/airframe integration on HWB system performance and engine operability across key on- and off-design conditions. The goal is to demonstrate an HWB propulsion airframe integration (PAI) design concept that will enable fuel burn reductions in excess of 50% (with 1% or less drag penalty) while providing noise shielding required to meet ERA noise reduction metrics (figure 1). NASA partnered with Boeing to design and verify an HWB PAI concept (see figure 2) that minimizes adverse

propulsion/airframe induced interference effects that could result in high drag or poor aerodynamic characteristics.<sup>1</sup> NASA and Boeing used computational fluid dynamics predictions (CFD) and a series of wind tunnel tests to: quantify key design trade space issues that impact UHB engine operability in HWB concepts and minimize the impact of adverse effects; characterize the impact of airframe dominated flows on the fan stall margin of a UHB concept; characterize the impact of propulsion induced flows on the performance and stability and control of an HWB configuration. A 5.75% scale model of the HWB concept was tested in the NASA LaRC 14- by 22-foot Subsonic Tunnel and the 40- by 80-foot test section of the National Full-Scale Aerodynamics Complex (NFAC) in a series of tests (figures 3 and 4): 1) A flow through nacelle test for aerodynamic assessment of the high lift system; 2) Powered ejector test to investigate inlet flowfields and distortion at the inlet face; and 3) Turbine Powered Simulator (TPS) test to assess power effects due to engine exhaust. The HWB concepts high speed cruise performance was evaluated using CFD.



Figure 2: Artist rendering of Boeing ERA HWB aircraft concept.



Figure 3: HWB model (flow-through nacelle configuration) installed in the NASA LaRC 14- by 22-foot Subsonic Wind Tunnel.



Figure 4: HWB FTN configuration installed in the NFAC 40- by 80-foot test section.

## I.A. Goals and Objectives

The purpose of ITD-51A is to advance the knowledge and Technology Readiness Level (TRL) of UHB engine integration on the HWB. UHB turbofans will also be evaluated for N+2 installations. These investigations need to address how to integrate a large diameter fan/nacelle with N+2 vehicle concepts. UHB turbofan engines have the greatest potential for meeting the noise goals, but need to address nacelle weight for large-diameter fans, viability of shorter inlets to reduce nacelle drag, thrust reversers, variable area nozzles and low-noise features of the fan. Variable area nozzles (or variable pitch fans) are needed for low-pressure ratio fans to maintain the desired operating line for sea level takeoff and cruise conditions.

Aircraft engines are the single most significant contributor to aircraft community noise. Virtually all of the large-scale installed engine airframe performance information comes from conventional tube-and-wing configurations with engine pods hanging below the wings.

Alternate configurations, such as hybrid wings with top-mounted engines and low-wing tube-and-wing concepts having over-the-wing mounted nacelles, may provide shielding benefits that offer tremendous potential to reduce community noise.

In the HWB configuration, the efficient integration of twin ultra-high bypass ratio turbofan engines will be critical to success from a performance (drag and stability and control), engine operability, and noise shielding perspective. The UHB Integration for HWB will address two major areas of interest in the development of this technology:

- **Aero Efficiency:** Details of actual engine integration such as nacelle size and location relative to oncoming flows (at cruise, and low speed conditions), vertical tails, and the aft deck are extremely important to interference drag effects as well as stability and control of an HWB configuration.
- **Engine Operability:** The operability of the inlets, fans, and nozzles resulting from the flow angularity driven by dominant flow-field features of an HWB configuration at low speeds, high angle of attack and crosswind operation must be examined before the HWB concept is considered a viable technology option for commercial transport vehicles.

ERA was managed by technical challenge. This ITD addresses the need to quantify the impact of engine/airframe integration on HWB system performance and noise across key on- and off-design conditions. This directly supports the ERA Technical Focus Area (TFA) on Airframe and Engine Integration Concepts for Community Noise and Fuel Burn Reduction and its Technical Challenge (TC) 5. TC 5 is defined as a demonstration of reduced component noise signatures leading to a value of 42 Effective Perceived Noise in Decibels (EPNdB) to Stage 4 noise margin for the aircraft system while minimizing weight and integration penalties to enable 50% fuel burn reduction at the aircraft system level.

The goal of the UHB Integration for HWB is to verify an HWB Propulsion Airframe Integration (PAI) design concept that will enable fuel burn reductions in excess of 50% while providing the noise shielding required to satisfy ERA noise reduction metrics.

The objectives of the UHB Integration for HWB were:

- Design the Advanced Vehicle Concept (AVC) HWB Preferred System Concept (PSC) to account for key critical off-design conditions (low speed, high angle of attack and sideslip, etc.) while maintaining excellent cruise performance.
- Characterize the performance (drag, lift, stability and control, propulsion induced effects, etc.) of the resulting HWB Propulsion Airframe Integration design throughout the Mach number range.
- Characterize the impact of propulsion induced flows on the performance and stability and control of an HWB configuration.
- Characterize the impact of airframe dominated flows on the operability of UHB engines at key off design conditions (low speeds, high angles of attack and sideslip) and minimize the impact of adverse effects.

## I.B. Preferred System Concept Aircraft Design

In phase I of the ERA project, a design study was undertaken to develop an aircraft to meet the ERA goals defined in figure 1. The resulting aircraft design was the ERA Hybrid Wing Body (HWB) Preferred System Concept.<sup>1</sup> To facilitate the technology demonstrations, Boeing completed a design update of the PSC configuration to support the development of the model scale HWB that was used in the subsequent wind tunnel test campaign.

Design refinements for the PSC were undertaken to address all the key performance metrics and ERA goals, but also to address the potential issues observed in the prior testing of HWB configurations. In 2012, an HWB configuration designated N2A-EXTE was developed by Boeing under NASA National Research Announcement (NRA). Low speed wind tunnel testing of the N2A-EXTE configuration revealed an issue with airframe generated inlet flow distortion - figure 5).<sup>2</sup> In addition, fundamental requirements for weight and balance, and stability and control were addressed in the updated PSC design. Boeing conducted the design revisions to the PSC in the areas of the planform, propulsion aerodynamic integration, high lift system, and propulsion system sizing and integration.

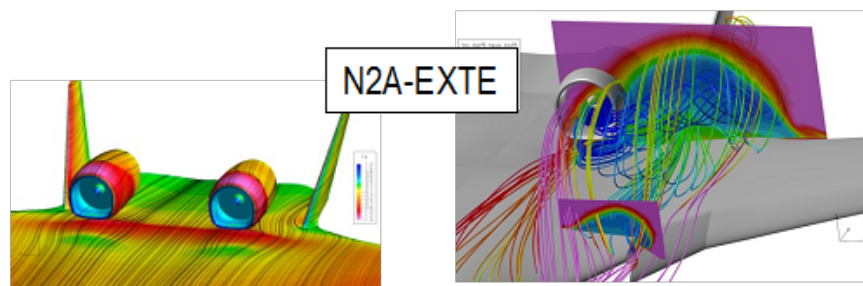


Figure 5: CFD simulations indicating inlet distortion on N2A-EXTE configuration.

Performance metrics addressed by the design included:

- Low Speed Inlet Distortion
- Low Speed Inlet Recovery
- Engine Installation Drag Penalty At Cruise
- Engine Position Relative To The Body Trailing Edge For Noise
- $C_{Lmax}$  at takeoff and landing
- Cruise Lift to Drag Ratio ( $L/D$ )

These design trades resulted in significant changes to the planform and wing leading edge sweep to improve stability and control and center of gravity characteristics of the aircraft (figure 6). Further, the integration of the propulsion system above the wing body presented challenges for both low-speed operability and high speed cruise drag. At high speed conditions there could be shock interactions between the nacelles as well as the body (figure 7). A rigorous optimization study was performed to minimize installed drag of the engine nacelle at transonic conditions. Further discussion can be found in the works by Bonet et al.<sup>3</sup> and Deere et al.<sup>4</sup>

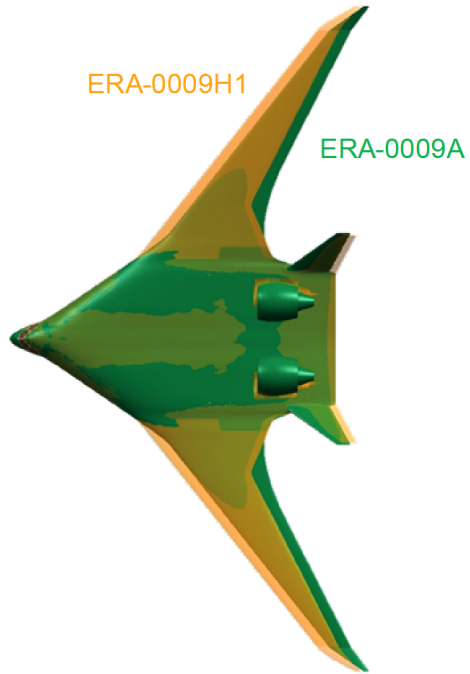


Figure 6: Evolution of the planform of ERA HWB from 0009A (green) to 0009H1 (orange, current) configuration.

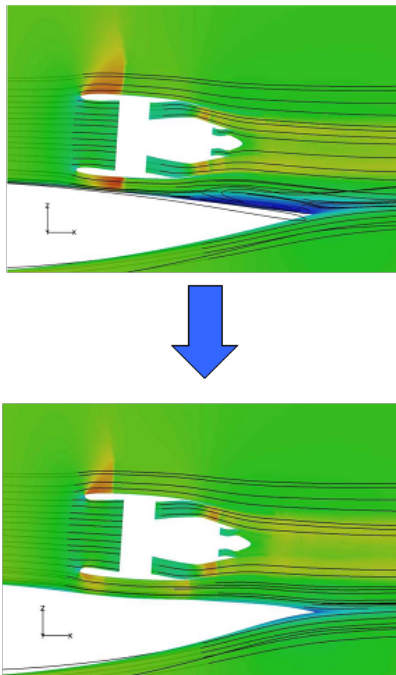


Figure 7: Nacelle and fuselage shaping reduce transonic drag - High speed predictions at Mach 0.85/43000 ft.

## II. Test Campaigns

To meet the objectives of the project, a series of wind tunnel test campaigns were conducted with three distinct model test configurations, HWB with flow through nacelles, HWB with ejector powered inlets, and HWB with turbine powered engine simulators. Force and moment testing was conducted on the model with a flow through nacelle configuration (figures 3 and 4).<sup>5</sup> Inlet distortion testing was conducted using an ejector powered engine inlets to simulate scaled inlet mass flows (figure 8).<sup>6</sup> Power induced effects on control surface effectiveness were studied with turbine powered simulators (TPS) to simulate scaled exhaust flow (figure 9).<sup>7</sup>

The first in the series of wind tunnel tests was conducted in the NASA LaRC 14- by 22-foot Subsonic Tunnel. This facility is a closed-circuit, single-return, atmospheric wind tunnel capable of producing a maximum speed of 348 feet per second. Further tunnel details and facility information are available in work by Gentry et al.<sup>8</sup>

As originally outlined, all wind tunnel testing for ITD-51A was to be done in the NASA LaRC 14- by 22-foot Subsonic Tunnel. Unfortunately, the facility experienced a failure of the main fan drive in September 2014 at the beginning of the first series of ejector test runs. The estimated amount of time to repair the motor was approximately one year. The delay would have extended the bulk of wind tunnel testing beyond the scheduled end of the ERA Project in September of 2015. A recovery plan was initiated to relocate subsequent testing to the National Full-Scale Aerodynamics Complex 40- by 80-foot test section at NASA Ames Research Center. Testing resumed at the NFAC 40- by 80-foot test section in January 2015. A description of the facility is available in the work by Hunt and Sacco.<sup>9</sup>



Figure 8: HWB model (ejector configuration) installed in the NFAC 40- by 80-foot test section.



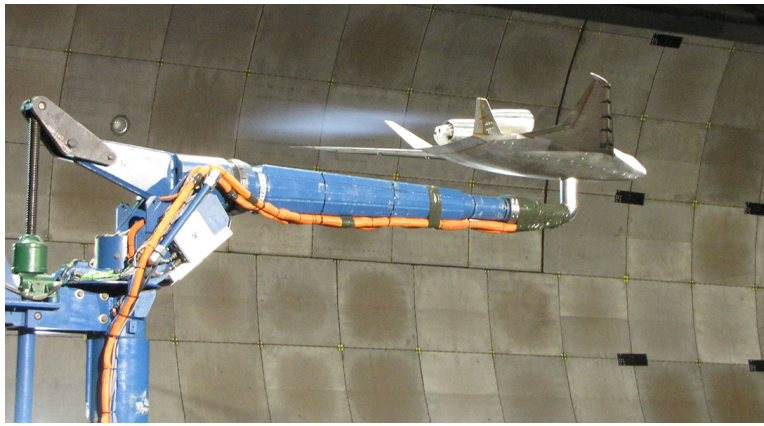


Figure 9: HWB model (turbine powered simulator configuration) operating statically in the NFAC 40- by 80-foot test section.

## II.A. Model Description

The model is a 5.75% geometrically scaled version of the Boeing Hybrid Wing Body designated ERA-0009GM configuration. Note that the outer mold lines for the model geometry were frozen in the first year of the project in order to fabricate the model hardware in time to meet testing milestones. However, the aircraft geometry was further refined by Boeing incorporating fuselage shaping discussed previously for transonic performance improvements resulting in the ERA-0009H1 configuration. The key difference between the ERA-0009GM (as tested) and the ERA-0009H1 is the fuselage shaping around the nacelles which was not expected to affect the subsonic performance characteristics of the aircraft. Basic model dimensions are given in table 1. A three-view drawing of the model is shown in figure 10. The model was instrumented with 331 pressure ports on the wing and main body and an additional 127 pressure taps on the inner and outer surface of the left hand nacelle and pylon. Forces and moments were measured using a six component flow through balance. The right hand nacelle in the FTN model was instrumented with a 40 probe rake. The ejector powered nacelles were instrumented with a 40-probe rake in the left hand nacelle and a 5-hole probe rake to measure swirl in the right hand nacelle. A full description of the model can be found in the work by Dickey et al.<sup>10</sup>

Table 1: Reference parameters for ERA ERA-0009GM test article.

Parameter	Dimension
Reference Area	26.833 ft <sup>2</sup>
Reference Span	12.228 ft
Mean Aerodynamic Chord	3.717 ft
Model Weight	1250 lbs

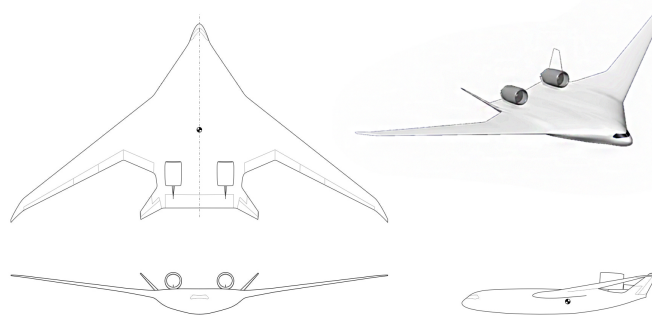


Figure 10: Three view of the ERA-0009GM

## II.B. Flow Through Nacelle Testing

The overall objective of the flow through nacelle testing was to define the high-lift system for take-off and landing conditions with the goal to optimize Krueger settings for high lift. Flow through nacelle testing was conducted in both the 14- by 22-foot Subsonic Tunnel and the NFAC 40- by 80-foot test section. Force and moment measurements were made using two different flow through balances: the newly constructed MC-126-6Ai balance and a lower capacity Ames 6 inch flow through balance No. 1. Data were obtained at dynamic pressures of  $q_\infty = 10, 20, 40, 60$  and  $90$  psf, with angle of attack sweeps up to very high  $\alpha$  beyond stall at varying angles of sideslip ranging from  $\pm 20^\circ$ . The majority of testing was conducted at a dynamic pressure of  $60$  psf. An extensive data set of leading edge Krueger deflection, gap and overhang characteristics was explored for both take-off and landing conditions (figure 11). A cruise configuration (no leading edge Krueger deflection) was also evaluated. From these data, the take-off and landing Krueger settings were selected and used in subsequent system analysis studies and follow-on inlet distortion and turbine propulsion-simulator tests. Figure 12 shows a sample data set with a Krueger angle of  $50^\circ$  for various gap and overhang settings. For this setting, the  $50^\circ(3,3)$  position (acoustic Krueger) with slot between wing and Krueger taped closed generally provided the best  $L/D$ . Further information can be found in the work by Vicroy et al.<sup>5</sup>

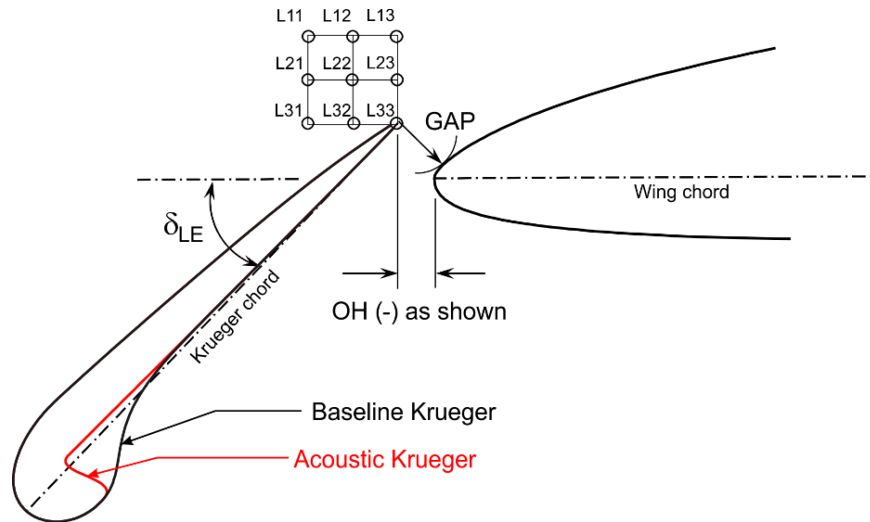


Figure 11: Krueger profiles and landing Krueger gap and overhang positions.

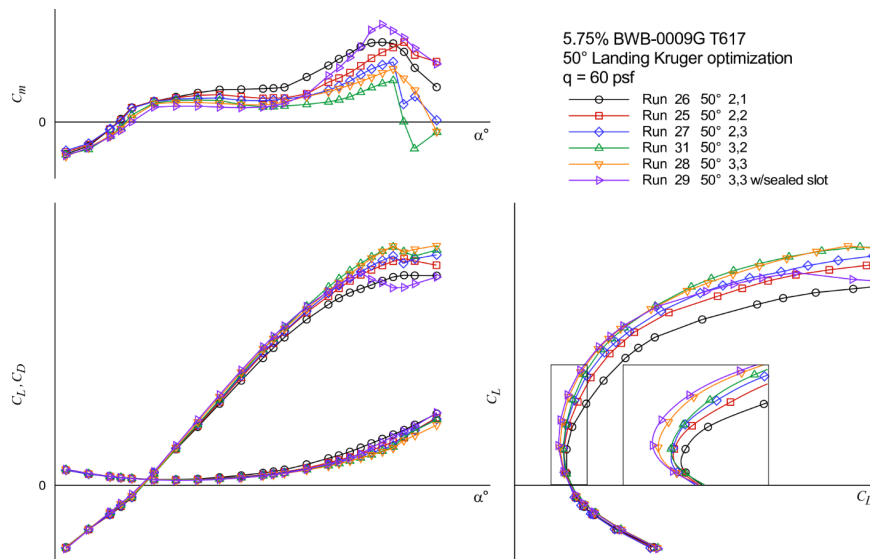


Figure 12: Landing Krueger measurements for  $50^\circ$  deflection.<sup>5</sup>

## II.C. Ejector Powered Inlet Testing

The objective of the ejector powered test was to characterize inlet flow distortion and to mitigate any adverse propulsion/airframe integration induced inlet flow distortion by parametrically varying inlet height and leading edge Krueger settings. With the aft body upper surface location of the engines, the inlets may be susceptible to vortex ingestion originating from the wing leading edge at high angles of attack and sideslip, and separated wing/body flow. The data obtained were used for engine operability characterization. For this test, the flow through nacelles were replaced by ejector powered inlets to simulate scaled mass flow conditions at the engine inlet (see figure 13). The ejector units used were two Tech Development Inc model 1900A ejectors. Initial data were obtained in the NASA LARC 14- by 22-foot Subsonic Tunnel. The tunnel main drive failed early in the ejector test campaign and all subsequent testing was conducted at the NFAC 40- by 80-foot test section at NASA ARC. Data were obtained at sweeps up to very high  $\alpha$  beyond stall at angles of sideslip ranging from  $\pm 45^\circ$ . The tunnel dynamic pressure,  $q_\infty$ , was set at 3.7, 6.2, 14.8, 33.3, and 59.2 psf which correspond to approximate Mach numbers of 0.050, 0.065, 0.100, 0.150, and 0.200, respectively. Inlet mass flow was varied from 4.54 to 7.62 lbm/s. A 40-probe rake mounted in the left inlet was used to obtain pressures for computing (see figure 13) inlet total pressure recovery ( $PR$ ) and inlet distortion intensity ( $DPCP$ ). A rotating swirl rake consisting of three arms with five 5-hole probes was mounted in the right hand inlet to take pressure measurements for computing swirl intensity. Preliminary analysis indicate a small vortex being ingested during engine spool up although distortion levels remained within acceptable limits. For more information see the work by Carter et al.<sup>6</sup>

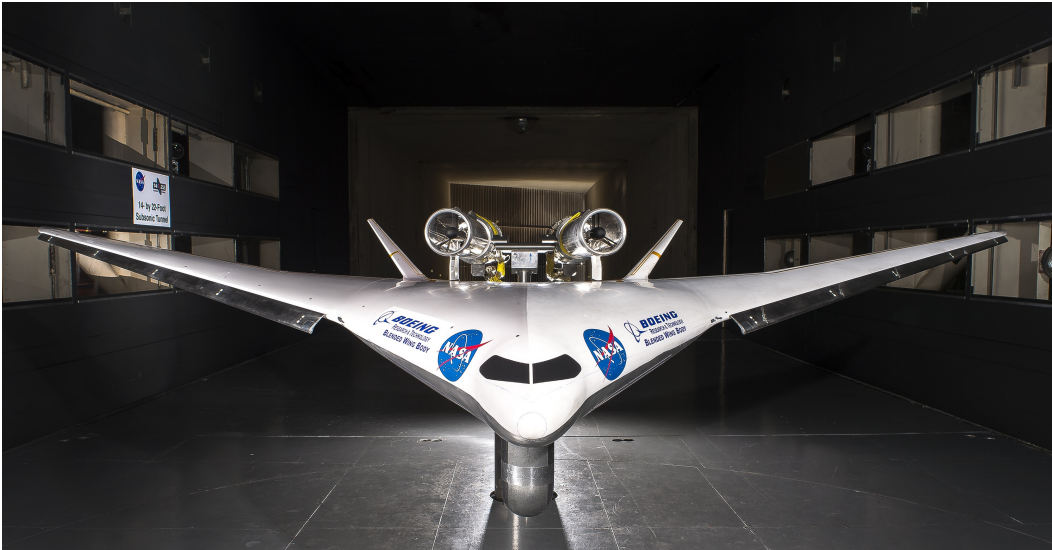


Figure 13: HWB model (ejector configuration) installed in the NASA LaRC 14- by 22-foot Subsonic Tunnel.

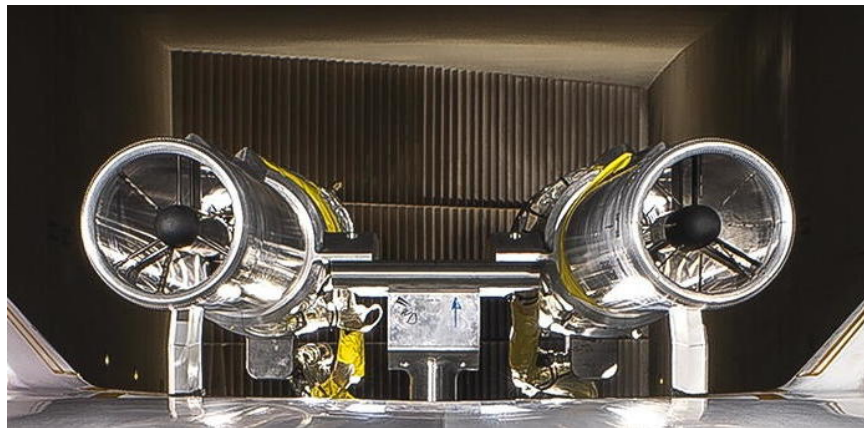


Figure 14: Close-up view of inlets and instrumentation rakes.

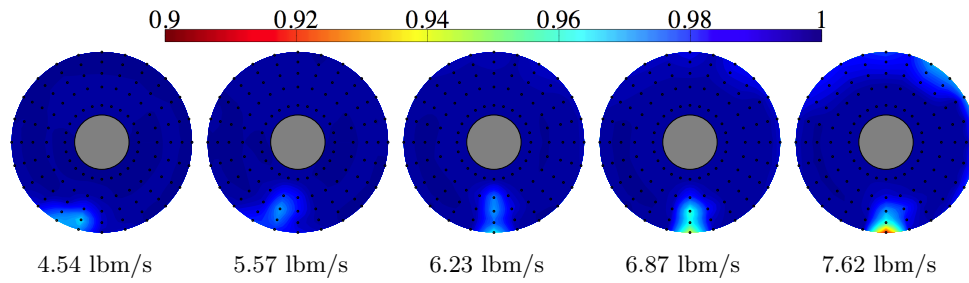


Figure 15: Effect of Mass flow rate on total pressure ratio at Mach 0.05,  $\alpha = 1^\circ$ ,  $\beta = 0^\circ$ .

#### II.D. Turbine Powered Simulator Calibration and Testing

The overall objective of the turbine powered simulators (TPS) powered test was to characterize the power-on effects of the engine exhaust flow and to increase pitching moment to enable take off rotation. For this test campaign, two Tech Development Inc, model 2700 TPS units were installed on the HWB model. The TPS units were previously modified to achieve a target mass flow of 7.77 lbm/s and Fan Pressure Ratio,  $FNPR$ , of 1.36 as described in the work by Tompkins.<sup>11</sup> The TPS test was conducted in the NFAC 40- by 80-foot test section at a  $q_\infty$  of 60 psf. Force and moment measurements were obtained using the NASA Ames 6 inch flow through balance No 1. Model angle of attack sweeps were completed up to  $20^\circ$  at model sideslips ranging from  $\pm 10^\circ$ . Three nominal engine power settings were tested at  $FNPR$  values of 1.04, 1.10 and 1.36 at three different center elevon deflections of 0,  $-30^\circ$ , and  $-40^\circ$  (deflected up toward engine exhaust). Two pylon heights were also tested. Figure 9 shows an image of TPS units installed on the HWB model and operating in the NFAC 40- by 80-foot test section. Data analysis of the wind-on TPS force and moment data is ongoing at the time of the writing of this paper.

The TPS units were calibrated prior to testing installed on the HWB in the NFAC. The individual TPS units were tested and calibrated statically in the NASA ARC Unitary Plan Wind Tunnel (UPWT) 9- by 7-foot Supersonic test section. A photo of the calibration test setup is shown figure 16. The TPS units were fitted with a calibrated bellmouth and tested with multiple exit nozzles of varying areas to develop operational fan maps of nozzle weight flows as a function of corrected fan rotational speed and fan pressure ratio. The TPS units were tested using the NASA Ames 6 inch Flow through Balance No 1. to develop thrust tables for use in wind-on testing on the HWB model. The work by Long et al.<sup>7</sup> further discusses the calibration and testing efforts of the TPS units on the HWB model.

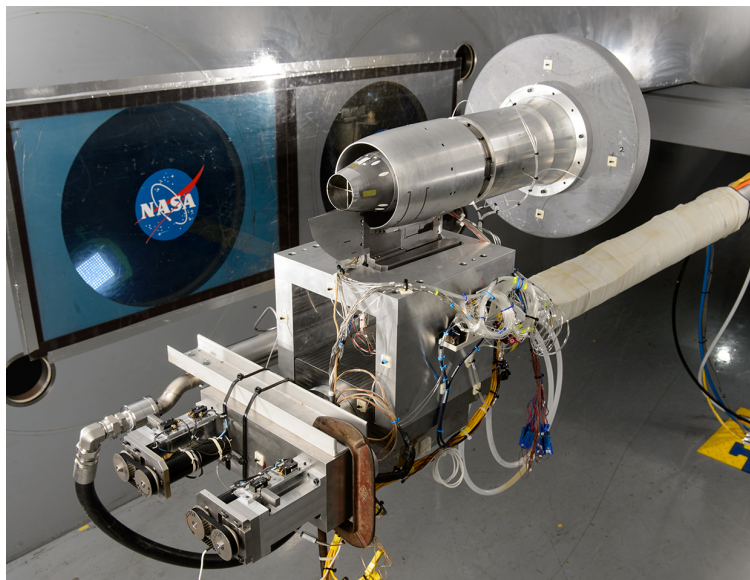


Figure 16: Calibration Setup of TPS Units in the NASA ARC UPWT 9- by 7-foot Supersonic test section.

## II.E. Phased Array Acoustic testing

As discussed previously, one of the system level metrics of the project was to demonstrate reduced component noise signatures leading to a value of 42 EPNdB to Stage 4 noise margin for the aircraft system (figure 1). The original project plan called for all of the noise estimates to be done computationally. No direct acoustic measurements of the HWB model were originally planned as part of the test program. However, the re-planning of the project to move to the NFAC 40- by 80-foot test section after the main drive failure in the 14- by 22-foot Subsonic Wind Tunnel afforded an opportunity to acquire experimental acoustic data to better refine noise estimates.

Experimental acoustic data were obtained on the HWB with the flow-through nacelles installed in the NFAC 40- by 80-foot test section. A new traversing array support was installed below the left wing of the HWB to measure Krueger flap noise for a number of configurations. Significant pre-test CFD resources were devoted to determining an acoustic array position that would yield high signal-to-noise ratios while not inducing significant aerodynamic effects on the test article. An acceptable location was determined with a wing to array separation distance for a  $90^\circ$  emission angle of 56.89 inches at  $\alpha = 0^\circ$  (which produces a separation of 111.57 inches at  $\alpha = 30^\circ$ ).<sup>12</sup> Figure 17 shows the array in different flyover positions. Data were acquired for a number of Krueger configurations, dynamic pressure sweeps ranging from 20 to 60 psf, angle-of-attack sweeps from 0 to  $16^\circ$ , and convected emission angles from 60 to  $120^\circ$ . Preliminary results show that Krueger noise is a strong function of gap size. The sealed gap configuration produced high-lift noise comparable to the baseline cruise configuration. The high-resolution beamform images showed the acoustic research team that Krueger brackets were the primary noise sources on the leading edge (figure 18). The acoustic array resolution was sufficient to distinguish between structural and flight-like brackets. For more information see the work by Burnside et al.<sup>13</sup>

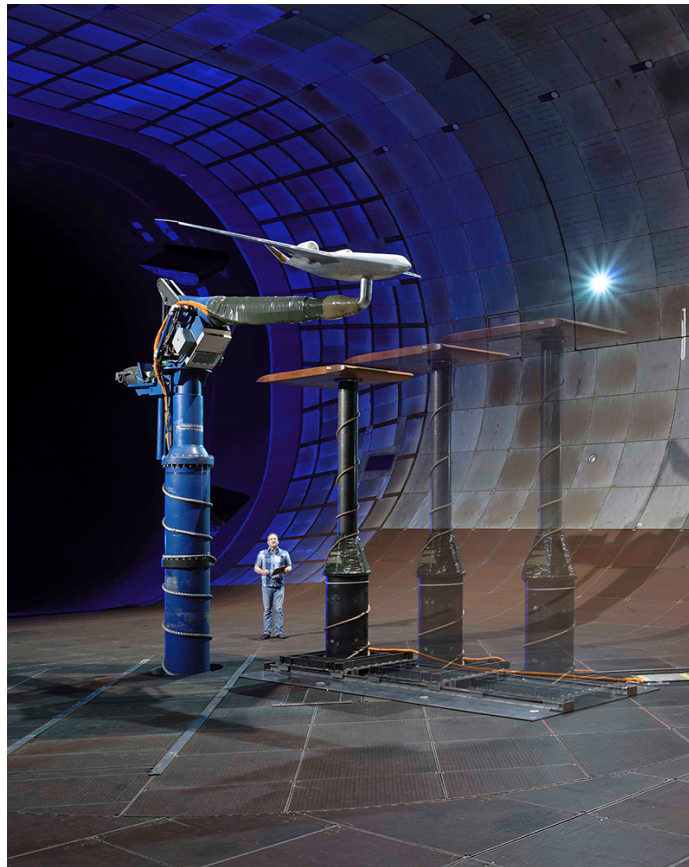


Figure 17: HWB FTN configuration installed in the NFAC 40- by 80-foot test section with phased array shown in 3 positions via multiple exposures.

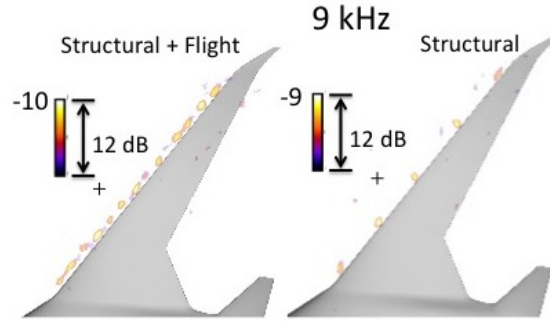


Figure 18: Krueger brackets are the dominate noise source at 9 kHz.<sup>13</sup>

### III. Computational Fluid Dynamics Assessments

#### III.A. Transonic Performance

An important part of validating that the Boeing design of the HWB meets fuel burn performance goals was to assess the vehicle’s transonic performance characteristics. In the original ITD-51A plan, this was to be accomplished using a combination of CFD and a high speed transonic wind tunnel test. However, several program constraints resulted in the elimination of the high-speed, transonic experimental testing portion of the project. Consequently, all high-speed, transonic performance characterization of the HWB design was done exclusively with CFD. In order to add confidence to the CFD predictions, two independent assessments were performed. NASA’s computations were performed using the NASA developed unstructured grid code USM3D. Boeing’s calculations were performed using the structured grid code OVERFLOW (modified by Boeing). Both codes are the fully turbulent, Reynolds-averaged Navier-Stokes flow solvers.

NASA also conducted an independent assessment of the transonic performance of the ERA-0009h. The goal was to assess Boeing’s overall process for determining interference drag and to develop a database of independent CFD solutions for comparison. In general, agreement between the two independent simulations was excellent. Drag coefficient was generally predicted to within one count (figure 19) for unpowered cases. Surface pressure contours on the wing and body were nearly identical (figure 20). Additional information is available in the works by Deere et al.<sup>4</sup> and Bonet et al.<sup>3</sup>

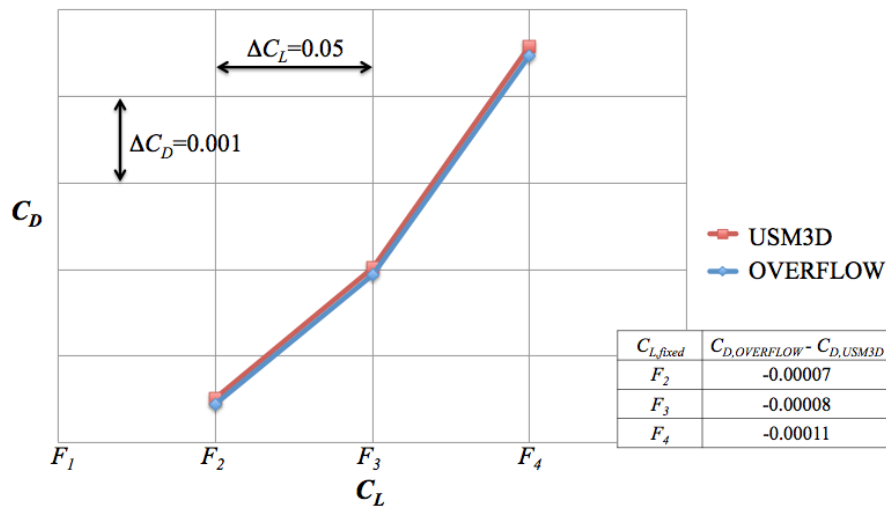


Figure 19: Comparison of  $C_D$  between USM3D and Boeing OVERFLOW for the HWB wing/body/tail configuration at  $M = M_8$  (cruise Mach) and  $C_{L, fixed} = F_2, F_3,$  and  $F_4$ . Where  $F_3$  is cruise  $C_L$ .<sup>4</sup>

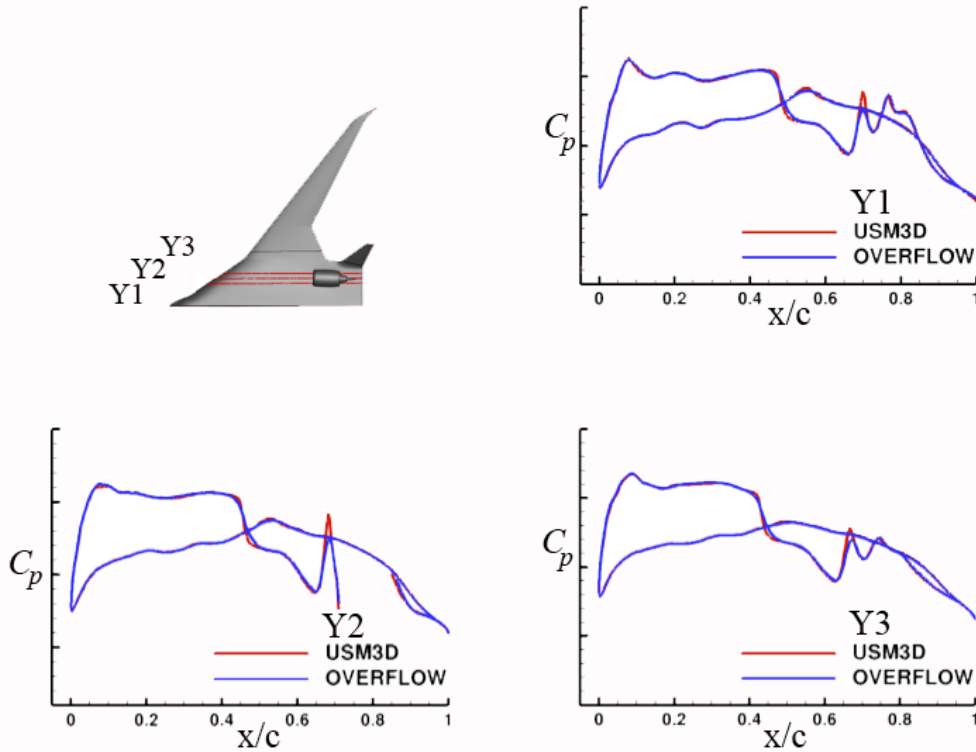


Figure 20: Comparison of  $C_p$  between the two codes at 3 stations on the body of the HWB wing/body/tail/nacelle/pylon configuration (no center elevon deflection) at  $M = M_8$ ,  $C_{L, fixed} = F_3$  (cruise conditions), and an engine power condition of  $Thrust = Drag$ .<sup>4</sup>

### III.B. CFD to support wind tunnel testing

As discussed in the introduction, one of the metrics of importance for ERA ITD-51A was a significant reduction in fuel burn. One of the primary data inputs to determine fuel burn is vehicle drag. To meet the levels of accuracy required to provide statistically meaningful data, vehicle drag needed to be determined to an accuracy of  $\pm 0.75$  lb (at  $q_\infty = 60$  psf). Levels of accuracy on that order for drag are difficult for a single configuration, run carefully in a single facility. However, ERA ITD-51A was tested in multiple configurations across two very different facilities with very different support systems. In order to achieve this, extensive computational analysis of the model support systems and facilities were made prior to the onset of testing.

CFD was used extensively for sting design and placement for both the wing body and powered ejector support structures and the placement of the aeroacoustic array to minimize their impact on the wind tunnel model aerodynamics. CFD was also used to compute wind tunnel wall interference corrections for both the LaRC 14- by 22-foot Subsonic Tunnel and NFAC 40- by 80-foot test section, cove design of the Krueger, and trip dot sizing for boundary layer transition. A more detailed discussion of the CFD conducted to support wind tunnel test campaigns can be found in the work by Garcia et al.<sup>12</sup>

As an example of how CFD was used to support testing, an early decision required to support the wind tunnel model design process in the project was to determine optimal sting support location on the model. CFD data were obtained on the effects of the sting support structure for the HWB model as installed in both the LaRC and the NFAC tunnels. Solutions were determined through the use of multiple codes (STAR-CCM, USM3D, and OVERFLOW) and a variety of turbulence models (see figure 21).

Four possible sting geometries were investigated: short-forward, short-aft, long-forward, and long-aft.

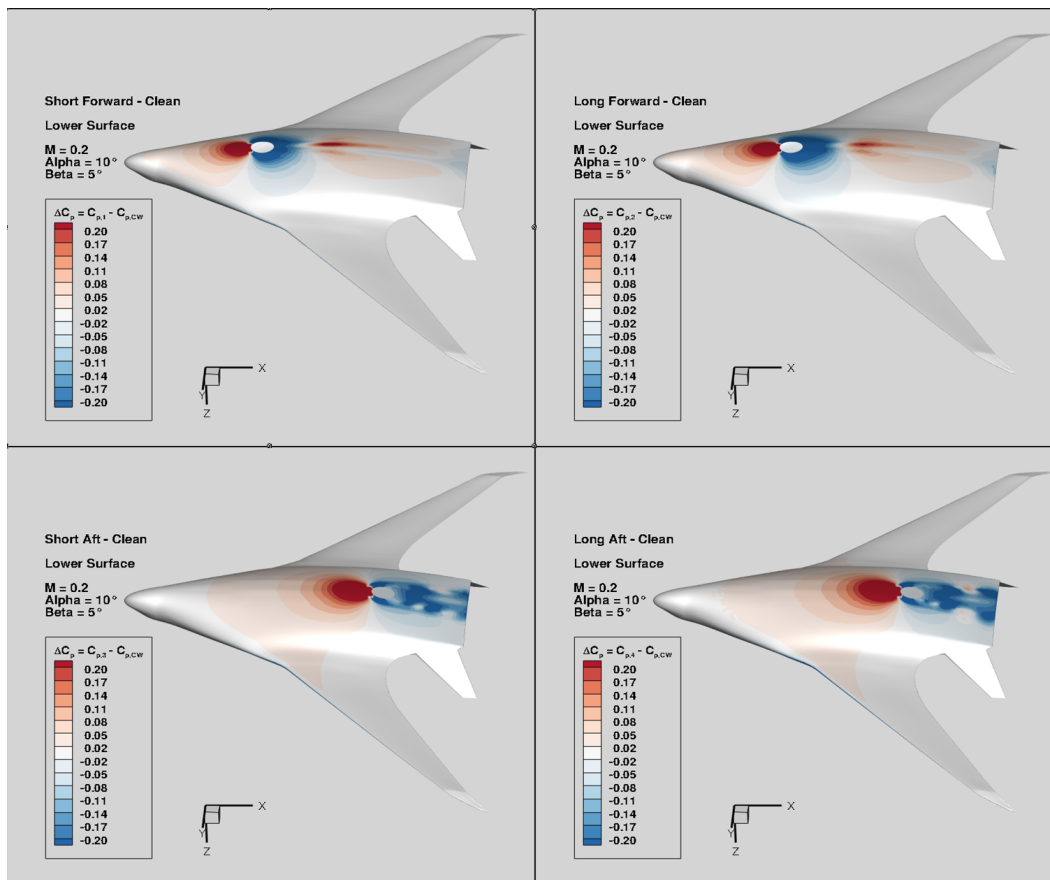


Figure 21: USM3D simulations showing effect of various sting configurations on lower surface pressure distributions.

The nomenclature refer to the length of the standoff (short vs. long) at the location that it penetrates the wind tunnel model lower surface and the location (forward vs. aft) that the penetration was to be made.

CFD solutions were made for most of the anticipated model configurations and many of the test conditions. These included:

- Clean wing configurations
  - $\alpha = 0, 8, 12, 14^\circ$  with  $\beta = 0^\circ$
  - $\alpha = 10^\circ$  with  $\beta = 2, 4, 6, 8, 12^\circ$
- Krueger
  - $\alpha = 15, 20^\circ$  with  $\beta = 0^\circ$

In determining which configuration had the least interference on the model, the differences due to the presence of the sting were examined for all forces, moments, and selected  $C_P$  distributions. Based on the observed effects the short-forward sting position was determined to have the least effect on the model test data.<sup>12</sup>

### III.C. Flow Through Nacelle Model Computational Assessment

Wind tunnel tests at both the NASA LaRC 14- by 22-foot Subsonic Tunnel and the Ames 40- by 80-Foot test section have been conducted on the Boeing HWB 0009GM configuration. These wind tunnel tests entailed various entries to evaluate the propulsion airframe interference including aerodynamic performance



and aeroacoustics. In order to baseline the powered configuration being tested, a simplified engine FTN configuration was tested as well. All models tested were 5.75% scale versions of a Boeing HWB configuration. A summary of CFD simulations from four different flow solvers that were conducted in advance of the FTN test in support of model integration hardware design as well as some post-test aerodynamic performance data comparisons for the FTN configuration.

CFD simulations were made in the months prior to testing this model in the NASA LaRC 14- by 22-Subsonic Tunnel and the NFAC 40- by 80-foot Test Section. The HWB model was tested in the 14- by 22-Subsonic Tunnel during July of 2014 and in the 40- by 80-foot test section during January and February 2015 and again during the June to August 2015 time period. Data was collected for the model in the FTN configuration during each of these test periods. CFD simulation predictions for four different codes, CFD++, OVERFLOW, STAR-CCM+, and USM3D and the wind tunnel test data for the FTN model in both the landing and cruise configurations were investigated. CFD predictions were made for the model in free air, free air with the wind tunnel sting, and in the wind tunnels with the sting and vertical support structures. Sample results for lift and drag for the model in a high-lift configuration are shown in figure 22 and figure 23. For additional results refer to the work by Schuh.<sup>14</sup>

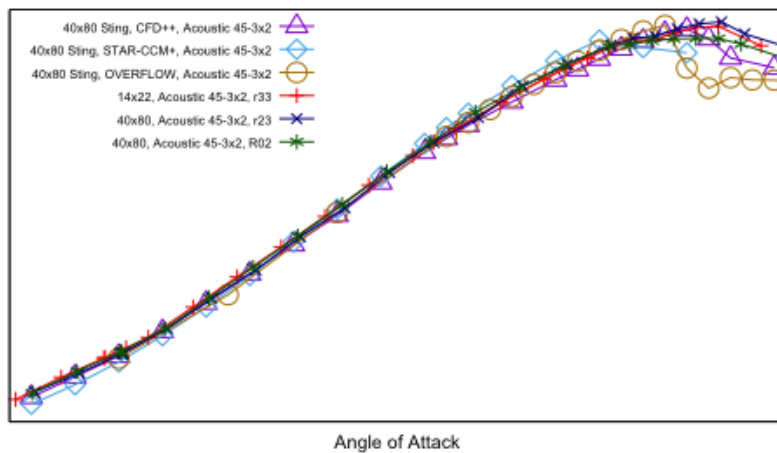


Figure 22:  $C_L$  for Acoustic Krueger 45-3x2 CFD, LaRC 14- by 22-foot Subsonic Tunnel, and ARC 40- by 80-foot test section fully corrected data for  $q_\infty=60 \text{ lb}_f/\text{ft}^2$ .

14

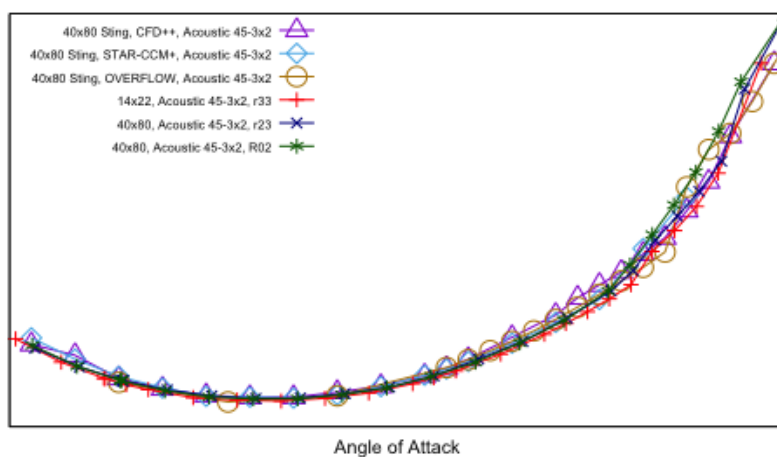


Figure 23:  $C_D$  for Acoustic Krueger 45-3x2 CFD, LaRC 14- by 22-foot Subsonic Tunnel, and ARC 40- by 80-foot test section fully corrected data for  $q_\infty=60 \text{ lb}_f/\text{ft}^2$ .

14

### III.D. Computational Assessment of Ejector Installation and Inlet Distortion

Due to the aft, upper surface engine location on the Hybrid Wing Body (HWB) planform, there is potential to shed vorticity and separated wakes into the engine when the vehicle is operated at off-design conditions and at conditions required for engine and airplane certification. CFD studies were conducted to assist with the planning of the test and to compare results with experimental data. CFD simulations were performed of the full-scale reference propulsion system, operating at a range of inlet flow rates, flight speeds, altitudes, angles of attack, and angles of sideslip to identify the conditions which produce the largest distortion and lowest pressure recovery. This data was used in engine operability assessments conducted by Pratt & Whitney. Pretest CFD was also performed by NASA and Boeing, using CFD++, OVERFLOW, and Star-CCM+. These data were used to make decisions regarding model integration, characterize inlet flow distortion patterns, and help define the wind tunnel test matrix. CFD was also performed post-test. When compared with test data, it was possible to make comparisons between measured model-scale and predicted full-scale distortion levels. An example computational result indicating a ground vortex developing off of the aft deck of the aircraft and being ingesting by the engine inlet is shown figure 24. This was also reflected in the experimental results as seen previously in figure 15. More detailed discussion can be found in the work by Tompkins and Sexton et al.<sup>15</sup>

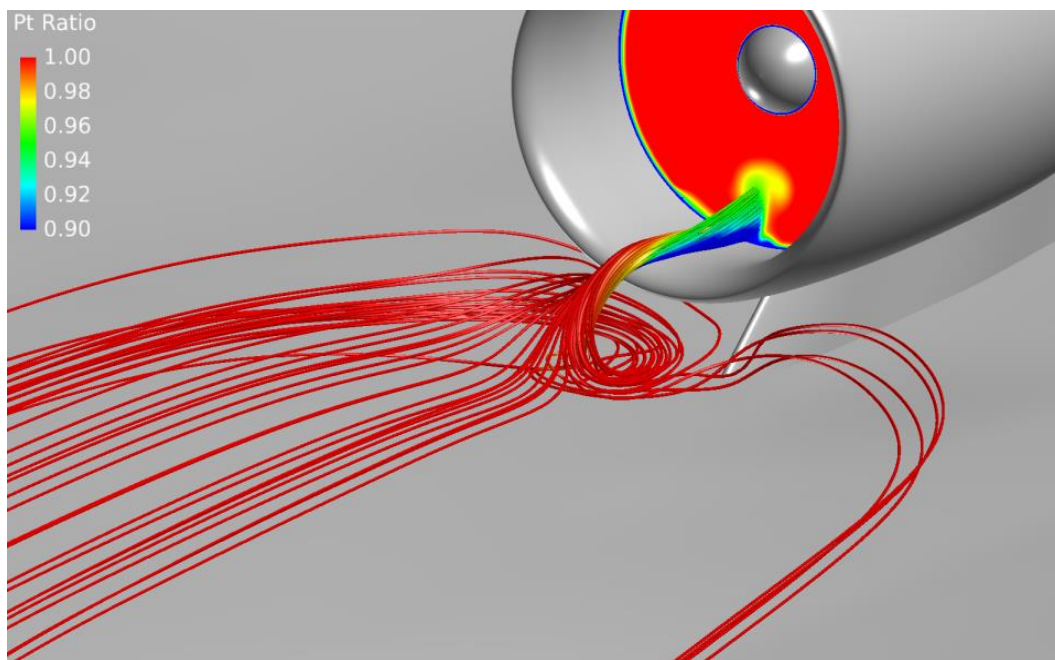


Figure 24: Computational results indicating vortex ingestion during ground roll at  $M = 0.05$ .

15

### III.E. Estimating Momentum Tares of Internal Air-flow Path for TPS testing

Propulsion simulation experiments at both the LARC 14- by 22-foot Subsonic Tunnel and the 40- by 80-foot test section have been conducted on a Boeing Hybrid Wing Body (HWB) configuration. These wind tunnel tests entailed various entries to evaluate the propulsion airframe interference including aerodynamic performance and aeroacoustics. High pressure air was ducted through the model support system, across the balance, and eventually exhausted through two turbine propulsion simulators. These small yet powerful air-driven turbines simulated the full scale engines and their high speed exhaust flows. CFD simulations were used extensively throughout the design and testing of the model. One critical element that was simulated was an estimation internal momentum tares of the flow through balance. These tares result from the internal flow of high pressure air through the balance's internal manifold (both frictional losses and the exchange of momentum when the flow is redirected through the various internal flowpaths), and must be subtracted from the net forces reported by the balance in order to isolate the external aerodynamic forces. A high level summary of the approach to the internal balance manifold CFD simulations using the flow solver was

STAR-CCM+ and limited comparisons with an experimental validation dataset are presented in the work by Melton et al. Figure 25 shows the CAD image of the internal air flow path for the TPS thrust calibration experimental setup and sample computational result showing internal pressures in the air supply path.<sup>16</sup>

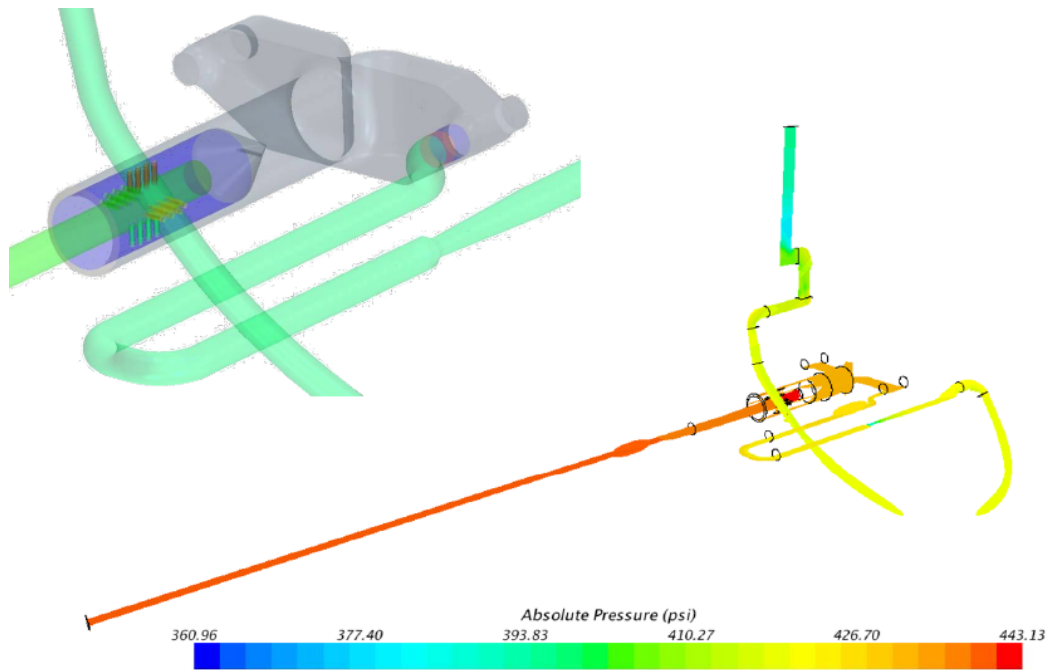


Figure 25: Geometry of the flow through balance as tested in the ARC UPWT 9- by 7-foot Supersonic test section.

16

#### IV. Engine Operability

An assessment of the impact of inlet distortion on engine and fan operability was performed by Pratt & Whitney using computational and experimental data obtained from the project . With the engines located at the upper aft fuselage of the HWB, there is the potential for flow distortion from the forebody to be ingested into the engines at high angles of attack, at aircraft wing stall several degrees past stall. The flow distortion could include both total pressure loss and flow angularity and swirl distortion. The distortion levels would be a function of the BWB forebody design including high lift devices as well as the aerodynamic operating condition i.e., Mach,  $\alpha$  and  $\beta$ . The potential threats to the engine were identified as fan stall, core engine (low pressure compressor) stall and fan blade vibratory stress. Some impact to engine performance would also be expected at any condition where there is significant inlet distortion, but that would represent an off-design condition and would not affect the mission fuel burn assessment. In this program the engine response to inlet distortion has been assessed based on analytical and empirical and computational simulation approaches. At this stage, the technology readiness level for the operability and blade stress assessment is approximately TRL 4. Boeing supplied data for inlet distortion at a number of limiting conditions that were derived from their CFD of the complete aircraft configuration at full scale, with inlet mass flow set to the nominal design table value for that flight condition and thrust level. The inlet flowfield data were provided at two axial stations within the inlet at the throat location and at the fan face. An example full aircraft solution and inlet distortion field mapped to fan inlet inflow boundary can be found in figures 26 and 27, respectively.<sup>3</sup>

For all the inlet distortion cases that were within the expected operational envelope of the PSC aircraft, the engine operability and fan blade stress metrics were determined to be within acceptable limits. Therefore, no modifications to the PSC engine design and system metrics from were deemed necessary.

Several inlet distortion analysis cases were considered that had more severe distortion than would be en-

countered within the operating envelope of the PSC aircraft. The operability assessment for these cases was either marginal or unacceptable. This result provided some additional confidence that the operability assessment methodologies were producing reasonable results. More detailed discussion of the engine operability assessment can be found in the work by Lord et al.<sup>17</sup>

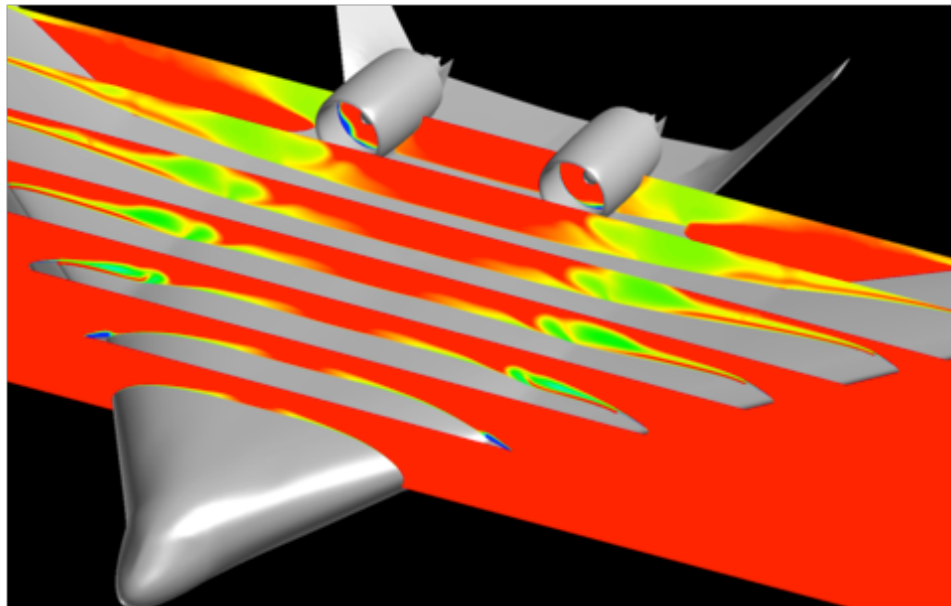


Figure 26: Sample full aircraft CFD++ solution used to assess engine operability.<sup>3</sup>

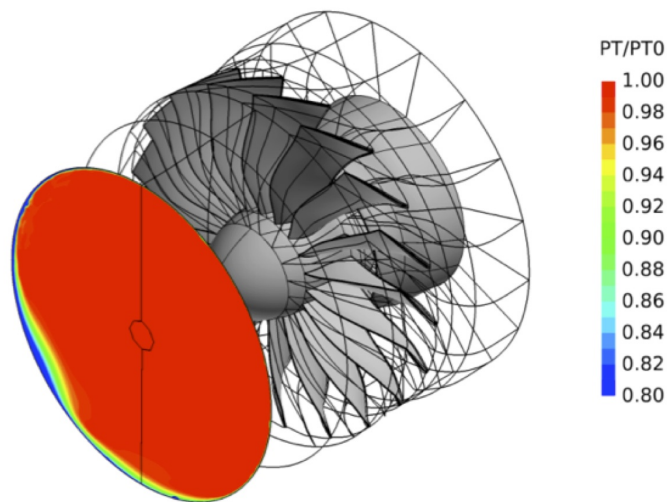


Figure 27: Sample CFD++ solution of inlet distortion mapped to fan face.<sup>3</sup>

## V. System Level Assessment

The ERA Phase II project goals are for simultaneously meeting mission fuel burn reduction of 50%, cumulative community noise levels of 42 dB below Stage 4, and 70% lower engine NOx emission. These vehicle level metrics remain valid measures of the technology maturation of the overall vehicle performance. Boeing made considerable design modifications to the PSC configuration, such as wing position, planform, and engine cycle and overall size. High fidelity analysis resulted in refinement to the aerodynamic lines of the nacelles, wing, body and control surfaces. The objective of the system level assessment is to quantify the overall integrated vehicle performance against the ERA project goals. A system level assessment was conducted for the updated ERA-0009H1 configuration with P&W Geared Turbofan engines installed. Results from the wind tunnel tests and other analyses were used to update the configuration. Design tradeoffs between noise reduction and fuel burn reduction were part of the system level assessment.

The changes to the PSC configuration resulted in the ERA-0009H1 achieving a fuel burn level that is more than 53% better than the reference configuration. The ERA-0009H1 has 1.8% lower fuel burn than the ERA-0009A, due primarily to the 5% increase in initial cruise  $L/D$ .

A certification noise level assessment for the PSC configuration ERA-0009H1 was made using the same methods as previous assessments. When landing gear fairing and chevron nozzle technologies are included on the vehicle, the cumulative margin below Stage 4 is 37.9 dB.<sup>3</sup>

## VI. Summary

The NASA Environmentally Responsible Aircraft Project ITD-51A: Vehicle Systems Integration, Engine Airframe Integration Demonstration has successfully concluded. This was a cooperative project between NASA and Boeing to design, build and test Boeing preferred system concept blended wing body aircraft ERA-0009H1 and assess its ability to meet ERAs N+2 (2020) goals. Specifically, the technology demonstration addressed the ERA technical challenge to *Demonstrate reduced component noise signatures leading to 42 EPNdB to Stage 4 noise margin for the aircraft system while minimizing weight and integration penalties to enable 50 percent fuel burn reduction at the aircraft system level.*

The NASA and Boeing team successfully planned and executed three wind tunnel tests of the ERA-0009H1 configuration; 1) A flow through nacelle test for aerodynamic assessment of the high lift system; 2) Powered ejector test to investigate inlet flow-fields and distortion at the inlet face; and 3) Turbine Powered Simulator (TPS) test to assess power effects of the engine exhaust flow. These data were used to assess the engine operability of UHB engines mounted on the upper surface of the aircraft and to optimize the high lift system to improve  $L/D$  and noise characteristics.

CFD was used extensively to refine the design of the HWB configuration to improve propulsion airframe integration overall drag at transonic conditions. CFD was also used extensively both pre- and post-test to guide model design and installation decisions and for comparison to test results.

Post test assessment of the HWB aircraft indicate that all inlet distortion cases within the operating envelope of the HWB allow for acceptable engine operability and blade stresses.

Systems assessments indicate that the ERA-0009H1 achieved a fuel burn level that is more than 53% better than the reference configuration. The certification noise level assessment concluded that the cumulative margin below Stage 4 is 38.4 dB when landing gear fairing and chevron nozzle technologies are included on the vehicle.

## References

<sup>1</sup>Bonet, J. T., Schellenger, H. G., Rawdon, B. K., Elmer, K. R., Wakayama, S. R., Brown, D. L., and Guo, Y., "Environmentally Responsible Aviation (ERA) Project – N+2 Advanced Vehicle Concepts Study and Conceptual design of Subscale Test Vehicle (STV) Final Report," NASA/CR-2011-216519.

<sup>2</sup>Gatlin, G. M., Vicroy, D. D., and Carter, M. B., "Experimental Investigation of the Low-Speed Aerodynamic Charac-

teristics of a 5.8-Percent Scale Hybrid Wing Body Configuration,” AIAA Paper 2012-2669, 30<sup>th</sup> AIAA Applied Aerodynamics Conference, 25–28 June 2012, New Orleans, LA.

<sup>3</sup>Bonet, J. T., Dickey, E., Princen, N., Sexton, M., Beyar, M., Tompkins, D. M., Kawai, R., Camacho, P., and Elmer, K., “Environmentally Responsible Aviation (ERA) Project ? Hybrid Wing Body Engine/Airframe Operability Testing Final Report,” NASA/CR-2015.

<sup>4</sup>Deere, K. A., McMillan, S. N., Luckring, J. M., Flamm, J. D., and Roman, D., “CFD Predictions for Transonic Performance of the ERA Hybrid Wing-Body Configuration,” 54<sup>th</sup> AIAA Aerospace Sciences Meeting, 4–8 January 2016, San Diego, CA.

<sup>5</sup>Vicroy, D. D., Dickey, E. D., Princen, N. H., and Beyar, M. D., “Reference Overview of Low-speed Aerodynamic Tests on a 5.75% Scale Blended-Wing-Body Twin Jet Configuration,” 54<sup>th</sup> AIAA Aerospace Sciences Meeting, 4–8 January 2016, San Diego, CA.

<sup>6</sup>Carter, M. B., Shea, P. R., Flamm, J. D., Schuh, M., James, K. D., Sexton, M. R., Tompkins, D. M., and Beyar, M. D., “Experimental Evaluation of Inlet Distortion on an Ejector Powered Hybrid Wing Body at Take-off and Landing Conditions,” 54<sup>th</sup> AIAA Aerospace Sciences Meeting, 4–8 January 2016, San Diego, CA.

<sup>7</sup>Shea, P. R., Flamm, J. D., Long, K. R., James, K. D., and Tompkins, D. M., “Turbine Power Simulator Calibration and Testing for Hybrid Wing Body Powered Airframe Integration,” 54<sup>th</sup> AIAA Aerospace Sciences Meeting, 4–8 January 2016, San Diego, CA.

<sup>8</sup>Gentry, G. L. J., Quinto, P. F., Gatlin, G. M., and Applin, Z. T., “The Langley 14- by 22-Foot Subsonic Tunnel: Description, Flow Characteristics and Guide for Users,” NASA Technical Paper 3008, 1990.

<sup>9</sup>Hunt, R. and Sacco, J., “Activation and Operation of the National Full-Scale Aerodynamics Complex,” AIAA Paper 2000-1076, 38<sup>th</sup> Aerospace Sciences Mtg., 10–13 January 2000, Reno, NV.

<sup>10</sup>Dickey, E. D., Princen, N. H., Bonet, J. T., and Ige, G. K., “Wind Tunnel Model Design and Fabrication of a 5.75% Scale Blended-Wing-Body Twin Jet Configuration,” 54<sup>th</sup> AIAA Aerospace Sciences Meeting, 4–8 January 2016, San Diego, CA.

<sup>11</sup>Tompkins, D. M., Long, K. R., Flamm, J. D., and James, K. D., “Experimental Validation of Modifications to a TDI Model 2700 Turbine Powered Simulator to Simulate a High-Bypass Ratio Engine,” AIAA Paper 2014-3888, 50<sup>th</sup> AIAA/ASME/SAE/ASEE Joint Propulsion Conference, 28–30 July 2014, Cleveland, OH.

<sup>12</sup>Garcia, J. A., Melton, J. E., Schuh, M., James, K. D., Deere, K. A., Luckring, J. M., Carter, M. B., Vicroy, D. D., Flamm, J. D., Stremel, P. M., Nikaido, B. E., Childs, R. E., and Long, K. R., “NASA ERA Integrated CFD for Wind Tunnel Testing of Hybrid Wing-Body Configuration,” 54<sup>th</sup> AIAA Aerospace Sciences Meeting, 4–8 January 2016, San Diego, CA.

<sup>13</sup>Burnside, N. J., Horne, W. C., Elmer, K. R., Cheng, R., and Brusnisk, L., “Phased Acoustic Array Measurements of a 5.75% Hybrid Wing Body Aircraft,” 54<sup>th</sup> AIAA Aerospace Sciences Meeting, 4–8 January 2016, San Diego, CA.

<sup>14</sup>Schuh, M., Garcia, J. A., Carter, M. B., Deere, K. A., Stremel, P. M., and Tomkins, D. M., “NASA Environmentally Responsible Aviation Hybrid Wing Body Flow-Through Nacelle Wind Tunnel CFD,” 54<sup>th</sup> AIAA Aerospace Sciences Meeting, 4–8 January 2016, San Diego, CA.

<sup>15</sup>Tompkins, D. M., Sexton, M. M., Mugica, E. A., Beyar, M. D., Schuh, M., Stremel, P. M., Deere, K. A., McMillin, S. N., and Carter, M. B., “Computational Evaluation of Inlet Distortion on an Ejector Powered Hybrid Wing Body at Takeoff and Landing Conditions,” 54<sup>th</sup> AIAA Aerospace Sciences Meeting, 4–8 January 2016, San Diego, CA.

<sup>16</sup>Melton, J. E., Long, K. R., James, K. D., and Flamm, J. D., “Estimating Flow-Through Balance Momentum Tares with CFD,” 54<sup>th</sup> AIAA Aerospace Sciences Meeting, 4–8 January 2016, San Diego, CA.

<sup>17</sup>Lord, W. K., Hendricks, G., Kirby, M. J., Ochs, S. S., Lin, R.-S., and Hardin, L., “Impact of Ultra-High Bypass/Hybrid Wing Body Integration on Propulsion System Performance and Operability,” 54<sup>th</sup> AIAA Aerospace Sciences Meeting, 4–8 January 2016, San Diego, CA.